ISSN 2229-5518

Finite Element Comparative Analysis of the Crushing Behaviour of Square Steel Tubes

Isaac C.W. [a*], Oluwole O.[b]

Abstract— The dynamic axial crushing of a thin-walled hot-rolled carbon steel square tubes are performed and their results were compared with published numerical and experimental data of a thin-walled high-strength steel. The goal is to determine and compare the mean crushing force, collapsed mode, energy absorption and crush force efficiency of the tube with respect to their different length sizes and impacting velocities using the commercial finite element Abaqus/Explicit package. The parameters used in this study are the peak crushing force, energy absorption, crush force efficiency (CFE) and specific energy absorption (SEA). The mild steel tube showed an increase in energy absorption with increased velocity of the striking plate. The overall crushing behavior of our models also showed a good correlation with experimental results.

Index Terms— Collapsed mode, Dynamic axial crushing, Energy absorption, Finite element, Thin-walled

1 Introduction

STRUCTURAL effectiveness and crashworthiness of vehicles, ships, pressure tanks and airplanes are increasingly becoming important for structural designers. In real situations, unstable responses are developed when dynamic loads are applied to structural members. Many experiments have been carried out to study the unstable response and behavioral characteristics of structural materials. To reduce design time, ensure better performance and optimization of the design, numerical simulations are performed for virtual testing of the experimental results. The numerical simulations can produce results without constructing a physical model which can be performed very quickly and with little or no cost implications. Road, rail and air accidents have continued to be a major concern. During this occurrence, large amount of kinetic energy are released which makes the accident to be fatal. To minimize this effect, thin-walled tubes are designed to convert the kinetic energy to plastic-strain energy. Schneider and Jones [1] conducted some experimental studies on quasi-static crushing and dynamic axial collapse of thin-walled high-strength steel structural sections and compared with mild steel sections. It was observed that a higher degree of effectiveness was found for mild steel spot-welded top-hat sections than for similar sections made from high-strength steel. Some authors have used the explicit time integration to find the crushing behavior of thin-walled steel tubes [2], [3], [4]. Kazanci and Bathe [5] used the implicit time integration for evaluating the crushing and crashing of tubes. They found out that implicit time integration solution is more suited than explicit time integration when solving low speed problems. Tarigopula et al. [6], [7] conducted both an experimental and numerical analysis of the axial crushing of thin-walled high-strength steel sections. Their results showed a decrease in absorption energy when the impacting velocity increased for the dynamic crash case. They also showed the influence of element formulation on the axial crushing of thin-walled dual-phase steel square section. Zhang et al. [8] investigated numerically a new type of collapsed mode that can absorbed more energy than the conventional square tubes. They included pattern to the tube and found that the initial peak force was reduced when compared to the conventional tube without pattern. Hosseinipour and Daneshi [9] performed both theoretical and experimental energy absorption and mean crushing load of thin-walled grooved tubes under axial compression. They found out that the quality and the quantity of the load-displacement curve and energy absorbed by the axial crushing of tubes could be controlled by the introduction of grooves with different distances. In recent years, increasing the energy absorption capacity and structural effectiveness of crushing tubes is becoming a major interest especially in crashworthiness study [10], [11]. While much work has been carried out on steel sections [12], very few authors have compared numerically the behavior of thin-walled high-strength steel and thin-walled mild steel with relation to their energy absorbing capacities, influence of impact velocity and their deformation modes. In this paper, the result of the mean crushing force, collapse mode, absorption energy and crushing force efficiency of the mild steel tube is compared numerically with the high-strength steel tube.

2 Model Geometry

The reference model geometry used for the numerical simulation and for comparing the three other models conform approximately to the test specimen geometry of the experiment as described in [6]. Fig. 1 shows the geometry of the model. An impacting mass of 600kg fixed in all directions except in the vertical downward displacement. Velocities of 5m/s, 10m/s and 15m/s were given to the impacting mass where the loading was applied, was used for all models. The rigid wall was fixed such that the whole degree of freedom was constrained. The tube thickness was constant for all geometries. Table 1 shows a summary of the geometrical parameter for all cases.

*Isaac Chukwuemeke William is currently pursuing a PhD degree program in the Dept. of Mechanical Engineering, University of Ibadan, Ibadan Nigeria
[a] Corresponding Author: E-mail: william.chuks@yahoo.com
[b] Dr. Oluwole Oluleke is currently a senior lecturer in the Dept. of Mechanical rtEngineering, University of Ibadan, Ibadan Nigeria.

ISSN 2229-5518

TABLE 1
GEOMETRICAL PARAMETERS FOR THE TEST SPECIMEN AND THE TEST MODEL IN MILLIMETRES

	Experiment (ds02) [6]	Implicit model [5]	Reference model	Model A	Model B	Model C
Breadth (b1)	59.7	59.7	58.9	58.9	58.9	58.9
Width (b2)	56.8	56.8	58.9	58.9	58.9	58.9
Thickness (t)	1.17	1.17	1.2	1.2	1.2	1.2
Radius (r)	3	3	3	3	3	3
Length (L)	311	310	310	175	264	350

3 MATERIAL PROPERTY

The square tube used for the finite element model was modeled as a strain rate sensitive material made from A36 steel hot rolled carbon. The effect of strain rate, strain hardening and thermal softening was taken into account using the Johnson-Cook constitutive isotropic hardening model [13] given as:

$$\sigma_T = \left[A + B\left(\varepsilon_{eff}^P\right)^N \left(1 + CIn\frac{\dot{\varepsilon}_{eff}^P}{\dot{\varepsilon}_0}\right)\left[1 - \left(\frac{T - T_0}{T_{melt} - T_0}\right)^M\right]\right] \quad (1)$$

where σ_T is the dynamic flow stress, ε_{eff}^P is the effective plastic strain, $\dot{\varepsilon}_{eff}^P$ is the effective plastic strain rate, $\dot{\varepsilon}_0$ is the reference strain rate, T, T_{melt} and T_0 are the initial, melting and transition temperatures respectively, A, B, C, N and M are material constant. The summery of the material parameters of (1) are shown in Table 2 with values for the specific heat C_p, Young Modulus E, density ρ and poisson ratio ν. The material property of the thin-walled high-strength steel section is given in [6].

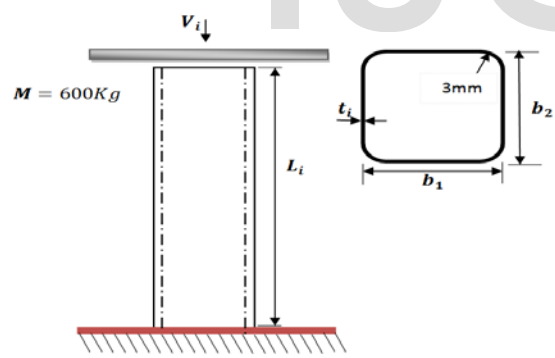

Fig. 1. Schematic of the model geometry. Where V_i is the initial velocity, L_i is the length of the tube, $b_1 = b_2$ is the width of the tube, t_i is the tube thickness and M is the impacting mass.

TABLE 2
MATERIAL PROPERTIES FOR THE A36 STEEL HOT ROLED CARBON

Parameter	Value
C_p(J/Kg°K)	486
T_{melt}(K)	1773
E(GPa)	200
$\dot{\varepsilon}_0$(s^{-1})	1
ρ(Kg/m^3)	7850
ν	0.26
A(MPa)	146.7
B(MPa)	896.9
C	0.033
N	0.320
M	0.323

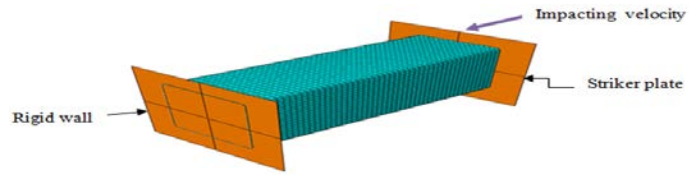

Fig.2. Finite element mesh of the square steel tube

4 NUMERICAL MODELING

The non-linear finite element code Abaqus/Explicit was used to predict the response of the thin-walled square tube which was subjected under axial crushing. Four different lengths of 174mm, 264mm, 310mm and 350mm were modeled with a cross-sectional perimeter of 240mm. The 310mm tube was used as a reference for virtual testing of the experimental solution of [6] and the numerical result of [5]. The result is then used as a reference for comparing the three other models. The type of finite element used for this study is the S4R element which is a three dimensional doubly curved four node shell element. A convergence study was carried out to determine the best appropriate mesh size. Table 3 shows the number of elements generated for three mesh sizes. Fig. 3 shows the effect of mesh refinement for the reference model of the dynamic crash case of 5m/s. it is seen that for the same step time of the reference model, an approximate global mesh size of 3.72 gives better result than the other two solutions. The tube was crushed axially between the impact plate and the rigid wall. Both the impact plate and the rigid wall were modeled using a three dimensional discrete rigid shell planer and does not need to be meshed as shown in Fig. 2. A general contact interaction was given to the tube which also takes care of the self interaction of the tube during deformation. The interactions between the impact plate and the rigid wall with the tubes were defined by a surface-to-surface contact with a friction penalty coefficient of 0.3. The dynamic loading conditions of different velocities for all geometries took less than 1200s total time step to run using a computer equipped with intel core i3 CPU at 2.2GHz.

5 MODELING PARAMETERS

5.1 Peak Crushing Force and Energy Absorption

The maximum load F_{max} required to cause a total distortion or a permanent change is the peak crushing force. It is the most important biomechanical factor which must be kept below the allowable value when designing an energy absorbing material [14]. The mean crushing force P_m is given by

$$P_m = \frac{1}{d}\int_0^{\delta} F(\delta)d\delta \quad (2)$$

where $F(\delta)$ is the instantaneous crushing load which corresponds to the instantaneous shortening δ. By Integrating the area under the load displacement curve, (2) gives the energy absorption E_a which is expressed as:

$$E_a = \int_0^{\delta} F(\delta)d\delta \quad (3)$$

ISSN 2229-5518

TABLE 3
ELEMENTS GENERATED FOR THE REFERENCE MODEL OF THE DYNAMIC CRASH CASE OF 5M/S

Mesh size	No. of elements generated
3.72	5644
4.00	4836
4.20	4440

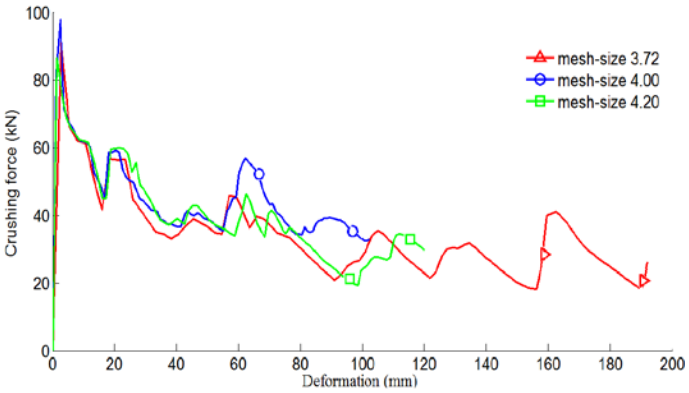

Fig.3. Effect of mesh-size refinement for the reference model of the dynamic crash case at 5m/s

5.2 Crushing Force Efficiency and Specific Energy Absorption

The ratio of the mean crushing force to the peak crushing force is the crush force efficiency denoted as:

$$CFE = \frac{P_m}{F_{\max}} \tag{4}$$

The higher the *CFE* the better the performance of the energy absorption structure [15]. A low *CFE* indicates high peak crushing force which could cause potential damages during impact. *CFE* is used to measure the structural effectiveness of vehicles and ships and should be kept high during structural design. Many authors have developed ways to increase the *CFE* such as using triggers [16], foam materials [17], etc. The energy absorbed per unit mass (m) is the specific energy absorption. It is denoted as:

$$SEA = \frac{E_a}{m} \tag{5}$$

This is a measure of the capability of different energy absorbed materials. By decreasing the absorber mass, high values of *SEA* can be obtained.

5.3 Structural Effectiveness

This is the ratio between the mean crushing force and the squash load. It is given as:

$$\eta = \frac{P_m}{A\sigma_T} \tag{6}$$

where A is the cross-sectional area of the thin-walled cross-section.

6 FINITE ELEMENT SIMULATION AND VALIDATION

In this section we give the results of the numerical solutions obtained using the Abaqus 6.10 package and compare them with the numerical implicit and experimental ds02, ds04, ds06 results.

6.1 Collapsed Mode

Fig. 4 shows the collapsed behaviour of the steel thin-walled hot-rolled carbon with that of the experiment of [6]. It is seen that this collapsed behaviour is slightly different from the collapsed behaviour of the experimental result due to the slightly different constitutive structure between the thin-walled hot-rolled carbon steel and the thin-walled high-strength steel. It is observed that the collapsed mode is affected by the speed of impact of the striker on the tube. Many time steps are required to obtain results with smaller impacting velocity. For smaller velocities the collapsed mode tends toward axisymmetric or concertina as observed by Han et al. [18]. As the impacting velocity approaches zero, the crushing behavior becomes quasi-static while at increasing velocities, irregularities were observed in the folding pattern as seen in Fig. 5. The relationship between the irregular folding pattern and the force-deformation curve for the highest impacting velocity of model *C* is depicted in Fig. 6.

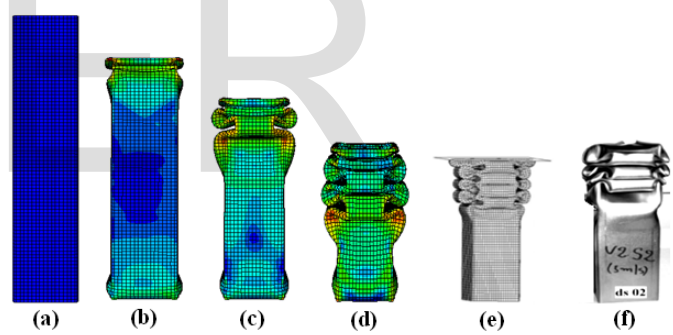

Fig.4. Deformation modes of the dynamic crash case at 5m/s: (a) (b) (c) and (d) are the reference model; (e) is the implicit model [5] (f) is the experimental specimen (ds02)[6]

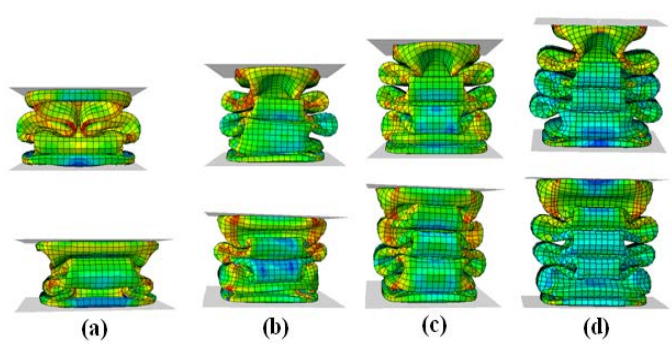

Fig.5. Final collapsed mode of the present model with impacting velocity of 15m/s for two side views: (a) L=176mm (b) L=264mm (c) L=310mm and (d) L=350mm

ISSN 2229-5518

6.2 Effect of Tube Length

The length of the tube affects both the absorbed energy and the mean crushing force. Table 4 shows the mean crushing force of the four different tube sizes with both the implicit result of [5] and the experimental result of [6]. Reduced tube length gives lower absorbed energy and produces higher peak crushing force while an increased tube length produce considerable higher absorbed energy as shown in Tables 4 to 6. It is therefore recommended to determine an appropriate tube size when designing an energy absorbing material. At velocity of 5m/s, only the deformation model *C* behaves like the reference model as depicted in Fig. 7. Model *A* and *B* only agree with the reference model at the peak crushing force.

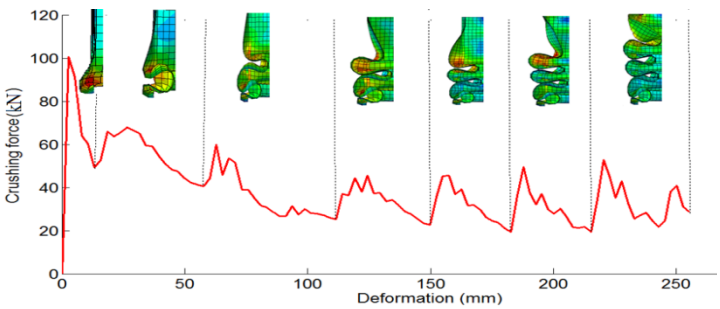

Fig.6. Relationship between mode shapes and the crushing force-deformation curve for model *C* at a velocity of 15m/s

TABLE 4
COMPARISON OF THE CRUSHING PARAMETERS FOR THE DYNAMIC CRASH CASE AT 5M/S

	Peak Force (kN)	Mean Force (kN)	Absorbed Energy (kJ)	CFE (%)
Experiment (ds02)	99	39.2	8.03	39.60
Implicit		36.4		
Reference model	91.35	32.70	6.28	35.80
Model A	97.83	36.45	3.19	37.26
Model B	97.72	46.54	3.94	47.62
Model C	95.35	33.94	6.44	35.60

TABLE 5
COMPARISON OF THE CRUSHING PARAMETERS FOR THE DYNAMIC CRASH CASE AT 10M/S

	Peak Force (kN)	Mean Force (kN)	Absorbed Energy (kJ)	CFE (%)
Experiment (ds04)	127	42.5	7.46	33.46
Implicit		40.1		
Reference model	105.12	37.35	8.59	35.53
Model A	117.34	40.34	4.89	34.38
Model B	103.35	43.10	7.99	41.70
Model C	101.95	36.91	8.49	36.20

TABLE 6
COMPARISON OF THE CRUSHING PARAMETERS FOR THE DYNAMIC CRASH CASE AT 15M/S

	Peak Force (kN)	Mean Force (kN)	Absorbed Energy (kJ)	CFE (%)
Experiment (ds06)	136	48.5	5.00	35.66
Implicit		43.2		
Reference model	105.14	39.28	9.36	37.36
Model A	129.28	41.18	5.73	31.85
Model B	114.59	41.03	8.04	35.80
Model C	100.57	37.61	9.60	37.40

6.3 Crushing Parameters

Tables 4 to 6 also show the results of the crushing parameters. The numerical results of the mean force agree considerably with the experiment (ds02, ds04, ds06) [6]. However, considerable higher peak forces were noticed in the experiment as the impacting velocity increases. Contrary to the decrease of the absorption energy with increasing impacting velocity as shown in the experiment, the absorption energy of all our models was observed to increase with increase impacting velocities. A reasonable agreement with the absorbed energy is observed for both the numerical model and experimental data for the dynamic crash case at 10m/s except for model *A* which is not as quite as close to the other results as seen in Fig. 8. The force-deformation behavior of our models as shown in Fig. 9 is slightly similar to one another which also agree with experimental result of [6].

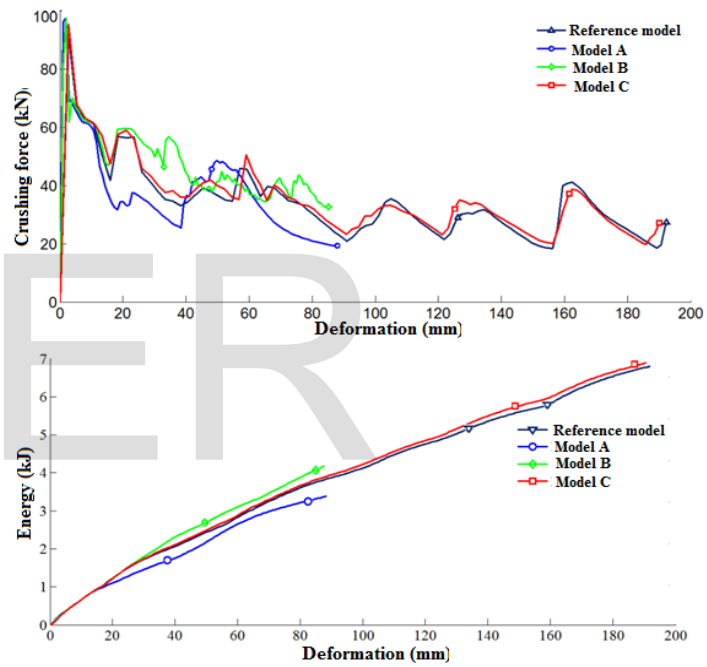

Fig.7. Comparison between the modeled square tube at 5m/s for both force-deformation and the corresponding energy curve

6.4 Energy Deformation Curve

Figure 7 to 9 show the corresponding absorbed energy-deformation curve. The models with increased length size give better energy absorbing capacity than those with reduced sizes. At velocities of 5m/s, 10m/s, and 15m/s, model *A* fully deformed by 51% , 71% and 80% respectively of its original length to produce an average absorbed energy of 4.6kJ. These results validate the work of Reid [19] who showed that for a thin-walled tube, more than one half of its length undergo plastic deformation.

6.5 Performance of the Model

The crushing force efficiency shows the performance of the crushed tube as seen in Tables 4 to 6. Model *B* gives the best performance of the crushed tube for both impacting velocity of 5m/s and 10m/s while model *C* is best suited when the impact-

ISSN 2229-5518

ing velocity is 15m/s. In general, there is a good agreement of the modeled crushed tube performance with that of the experiment.

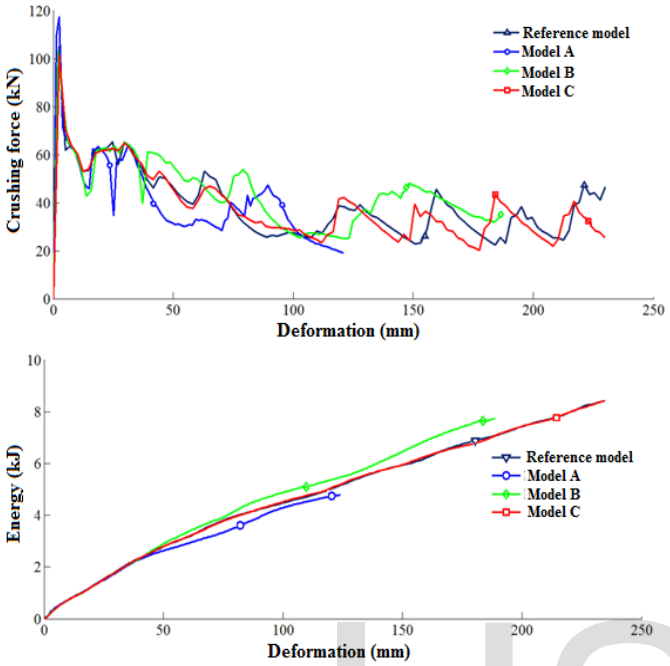

Fig.8. Comparison between the modeled square tube at 10m/s for both force-deformation and the corresponding energy curve

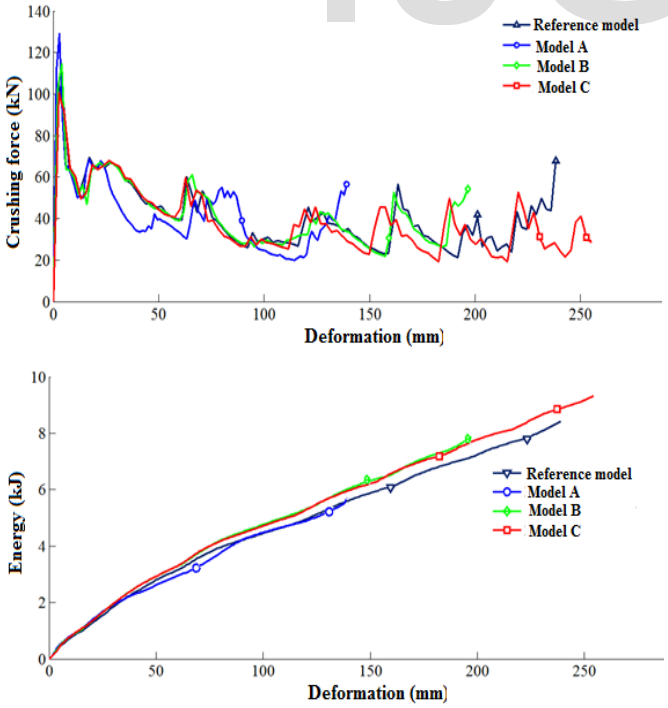

Fig.9. Comparison between the modeled square tube at 15m/s for both force-deformation and the corresponding energy curve

7 Conclusion

An explicit finite element analysis of a square mild steel tube with different length sizes has been model, analyzed and compared with established experiments and implicit solution. The study showed that the absorbed energy of a thin-walled tube can be affected by the type of materials used and its constitutive equation. In our study, a mild-steel tube with Johnson-Cook material property gives higher absorbed energy as the impacting velocity increases and with increased tube length while the experiment that used a high-strength steel material showed a decrease in absorbed energy as the impacting velocity increases. The crush force efficiency and the mean crushing force of the models agree considerably with the established experimental results.

References

[1] F. Schneider and N. Jones, "Impact of thin-walled high-strength steel structure sections," *Proc of the institutions of Mechanical Engineers, Part D. Journal of Automobile Engineering*, vol. 218, no. 2, pp. 131-58, 2004.

[2] M.M. Younes, "Finite element modeling of crushing behavior of thin tubes with various cross-sections," *International Conference on Aerospace Sciences and Aviation Technology*, vol.13, pp. 7-19, May 2009.

[3] A.A ljawi, M Abd-Rabou and S Asiri, "Finite element and experimental analysis of square tubes under dynamic axial crushing" *European Congress on Computational Methods in Applied Sciences and Engineering* pp. 1-13, 2004.

[4] F. Tarlochan and F. Samer, "Design of thin wall structures for energy absorption applications: design for crash injuries mitigation using magnesium alloy", *International Journal of Research in Engineering and Technology*,vol. 2, no. 7, pp. 24-36, Jul. 2013.

[5] Z. Kazanci, K. Bathe, "Crushing and crashing of tubes with implicit time integration", *International Journal of Impact Engineering*, vol. 42, pp. 80-88, 2012.

[6] V. Tarigopula, M. Langseth, O.S. Hopperstad and A.H. Clausen, "Axial crushing of thin-walled high-strength steel sections", *International Journal of Impact Engineering*, vol. 32, no. 2006, pp. 847–882, Jun. 2005.

[7] V. Tarigopula, M. Langseth, O.S. Hopperstad and A.H. Clausen, "Influence of element formulation on the axial crushing of thin-walled dual-phase steel square section", *International LS-DYNA user Conference*, pp. 16-13 to 16-20, Simulation Technology, 4.

[8] X. Zhang , G. Cheng, Z. You and H. Zhang, "Energy absorption of axially compressed thin-walled square tube with parttern" *Thin Wall Structure*, vol. 45, pp. 737-746, 2007.

[9] S.J. Hosseinipour and G.H. Daneshi, "Energy absorption and mean crushing load of thin-walled grooved tubes under axial compression", *Thin-Walled Structures* vol. 41, pp. 31-46, 2003.

[10] J. Van Slycken, P. Verleysen, J. Degrieck, J Bouquerel, B.C. De Cooman "Crashworthiness characterization and modelling of high-strength steels for automotive applications" *Proc. of the Institution of Mechanical Engineers, Part D: Journal of Automobile Engineering*, vol. 220, no. 4, pp. 391–400, 2006.

[11] S. Furusako, A Uenishi and Y Miyazaki, "Improvement of crashworthiness by application of high-strength steel" Nippon Steel Technical Report, (35-38)-95, Jan. 2007.

[12] P. Oscar and R. Luis Eduardo, "Impact Performance of Advanced High Strength Steel Thin-Walled Columns" *Proc. of the World Congress on Engineering*, pp. 1-6, Jul. 2008.

[13] R. Johnson and W. H. Cook, "A constitutive model data for metals subjected to large strains, high strain rates, and high temperatures" *Proc. of the 7th International Symposium on Ballistics, The Hague, Netherlands*, pp. 541-547, 1983.

[14] R. Emami, E. Alavi Moghadam, "Crashworthiness optimization of thin-walled cylindrical tubes with annular grooves under axial compression", *Article in advanced materials research*, pp. 1-6, Jan. 2011, doi:10.4028/www.scientific.net/AMR.463-464.30.

[15] C.S. Yuen, G.N. Nurick and R.A. Starke, "The energy absorption characteristics of double-cell tubular profiles", *Latin American Journal of Solids and Structures*, vol. 5, pp. 289-317, 2008.

[16] F. Samer, F Tarlochan, H Samaka and K Khalid, "Improvement of energy absorption of thin walled hexagonal tube made of magnesium alloy by using trigger mechanisms", *International Journal of Research in Engineering and Technology*, vol. 2, no. 10, pp. 173-180, Oct. 2013.

[17] A. Hanssen, M. Langseth and O. Hopperstad, "Static and dynamic crushing of square aluminium extrusions with aluminum foam filler" *International Journal of Impact Engineering*, vol. 24, no. 4, pp. 347-383, 2000.

[18] H. Han, F. Taheri and N. Pegg, "Quasi-static and dynamic crushing behaviors of aluminum and steel tubes with a cutout", *Thin Walled Structures*, vol. 45, pp. 283-300, 2007.

[19] Reid S.R. Plastic deformation mechanisms in axially compressed metal tubes used as impact energy absorbers. *International Journal of Mechanical Science,* vol. 35, no. 12, pp. 1035-1052, 1993.